Measurement of Heat Quantity in a Small Cusp-Type Direct Energy Converter for Divertor Thermal Load Reduction

Nonda, Yuya ; Yamada, Hirotaka ; Kitahara, Yuki ; Ichimura, Kazuya ; Nakamoto, Satoshi ; Takeno, Hiromasa ; Matsuura, Hiroto ; Nakashima,…

(Citation)
Plasma and Fusion Research,13:3405050-3405050

(Issue Date)
2018

(Resource Type)
journal article

(Version)
Version of Record

(URL)
https://hdl.handle.net/20.500.14094/90005264

Measurement of Heat Quantity in a Small Cusp-Type Direct Energy Converter for Divertor Thermal Load Reduction*)

Yuya NONDA, Hirotaka YAMADA, Yuki KITAHARA, Kazuya ICHIMURA, Satoshi NAKAMOTO, Hiromasa TAKENO, Hiroto MATSUURA[1)] and Yousuke NAKASHIMA[2)]

Graduate School of Engineering, Kobe University, Kobe 657-8501, Japan
[1)]*Radiation Research Center, Osaka Prefecture University, Sakai 590-8570, Japan*
[2)]*Plasma Research Center, University of Tsukuba, Tsukuba 305-8577, Japan*

(Received 28 December 2017 / Accepted 28 March 2018)

Divertor thermal load is one of the significant problems for a tokamak fusion device, and reduction of the thermal load is required. An application of a Cusp-Type Direct Energy Converter (CuspDEC), which is the device for D-^{3}He fusion power generation to separate charged particles and convert their energy directly into electricity, was proposed to mitigate the heat flux of the divertor plasma. In order to install the CuspDEC in the narrow divertor region, a small-size CuspDEC simulator equipped with permanent magnets (PM-CuspDEC) was constructed to demonstrate divertor simulation experiment in GAMMA 10/PDX, and the performance of charge separation was examined. On one hand, development of measurement technology of heat quantity was also researched. A new calorimeter (CM) made for suppressing heat transmission has newly been manufactured to measure the small energy of end-loss flux in GAMMA 10/PDX experiment. The CM consists of a copper plate and thermocouples and can measure heat quantity and an inflow current simultaneously. The composed new CM is installed in the PM-CuspDEC, and its performance is investigated. A helium ion is used in the experiment of measuring heat quantity. The CM has successfully worked and measured the slight variation of the temperature.

Keywords: divertor, heat flux, direct energy conversion, calorimeter, CuspDEC

DOI: 10.1585/pfr.13.3405050

1. Introduction

In a tokamak fusion reactor, the surfaces of divertor plates are exposed to a large thermal load estimated to exceed 10 MW/m^2, and to reduce the thermal load of divertor plates is one of the significant subjects. An application of Cusp-type Direct Energy Converter (CuspDEC) was proposed as a method to reduce the energy of divertor plasma [1]. The CuspDEC was originally proposed for D-^{3}He fusion power generation, by which charged particles were separated and their energy was directly converted into electricity [2]. Although the conventional CuspDEC is focused on cylindrical geometry, it can also be applied to Tokamak devices. For example, one of the possible ways to create the cusp magnetic field is to add coils under the divertor region just like snowflake divertor. When the CuspDEC is installed in the divertor, ions and electrons of the divertor plasma are separated by cusp magnetic field, and they flow into individual divertor plates. The thermal load could be mitigated due to deceleration by appropriately biased divertor plates according to each particle's energy and polarity.

In order to realize this approach, the CuspDEC should be settled at the divertor region, so miniaturization of the device was studied because divertor region was narrow. Permanent magnets (PMs) were employed [3], and a small size simulator (PM-CuspDEC) was constructed for divertor simulation experiments on GAMMA 10/PDX [4, 5]. In the test experiments of the PM-CuspDEC, however, the performance of charge separation in the device was not enough, and some revisions such as increasing the number of magnets and designing a coil-based structure [6] were examined. On one hand, development of measurement technology of heat quantity in the CuspDEC system was also researched. In GAMMA 10/PDX experiments, an initial stage will be performed by using usual end-loss flux of GAMMA 10/PDX. The energy of the end-loss flux is much smaller compared with that of E-divertor, so high sensitivity is required for the heat sensor. A prototype calorimeter (CM) was manufactured, which had a function to measure an inflow current simultaneously. It was tested by using a high energy ion beam, and it was also demonstrated that the thermal load was reduced by applying deceleration field [7].

In this paper, we developed a new CM following to the research of Ref. 7. The new CM is designed to improve sensitivity by suppressing heat transmission. The composed new CM is installed and tested for investigating its behavior by using a helium ion in the PM-CuspDEC.

author's e-mail: takeno@eedept.kobe-u.ac.jp

*) This article is based on the presentation at the 26th International Toki Conference (ITC26).

2. Experimental Setup

2.1 PM-CuspDEC experimental device

The PM-CuspDEC experimental device is schematically shown in Fig. 1, which shows radial-axial planes. Plasma flows along with axial direction. As shown in this figure, the device consists of two magnetic coils, A and B, and four cylindrical permanent magnets, and a CM. The CM is installed at the downstream of the device. The CM has a function to measure not only heat quantity but also an inflow current simultaneously. The principle of measurement is described in Sec. 2.2. The coil currents I_A and I_B have the same direction. The magnetic field created by I_A is used for plasma production and has a function to guide the plasma to the downstream of the device. The coil current I_B also creates a magnetic field. There exist two cusp magnetic fields at both ends of the magnet. When the magnetic field by the appropriate coil current I_B is superposed on those cusp fields, the cusp of the upstream is cancelled, and that of the downstream still remains. The typical structure of magnetic field in the PM-CuspDEC is shown in Fig. 2. Electrons are deflected by the cusp magnetic field, while ions go straight. The shape of the magnetic fields and the orbit of particles can be controlled by changing I_B.

The used gas for the experiment of measuring heat quantity is helium. The plasma is generated by the RF power source operated by a continuous pulse with a duty ratio of 0.5. The helium ions are extracted by an extraction voltage V_{ex} applied to the extraction electrode and reach the CM, when V_{ex} determines the energy of the ion. A DC bias voltage $V_{bias} = -50$ V (fixed) is applied to the CM to collect the ions and reflect the electrons.

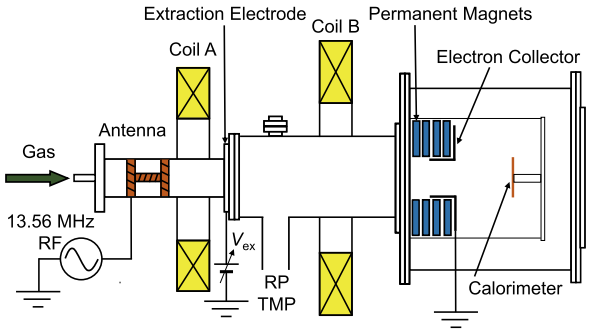

Fig. 1 Schematic image of the PM-CuspDEC experimental device.

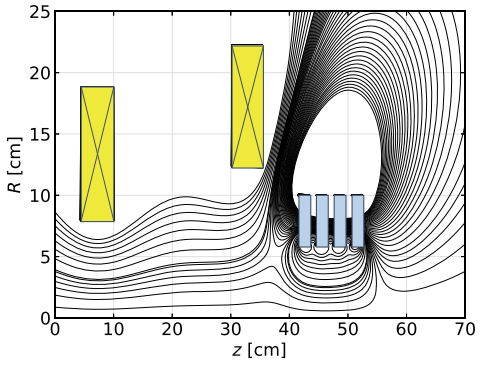

Fig. 2 The typical structure of magnetic field in the PM-CuspDEC.

2.2 Calorimeter

In GAMMA 10/PDX experiments, the end-loss flux will be used. The energy of the end-loss flux is smaller compared with that of E-divertor. So, heat sensor requires high sensitivity. A prototype CM was manufactured and was investigated its behavior by using a high energy helium ion beam [7]. Since the CM is observing a temperature of the target plate, thermal losses should be considered. Ref. 7 shows that the loss of the energy increases approximately 6 mW as the temperature difference rises by 1 kelvin. In the PM-CuspDEC, a new CM which is more sensitive to temperature change than the prototype one is needed because the energy of the incident heat flux is estimated to be on the order of 1 mW. It has been assembled to suppress heat transmission.

The schematic design of the CM is shown in Fig. 3. The new CM consists of a copper target plate, a thermocouples (TC) of chromel-constantan (E-type), and a nylon spacer. The TC with SUS sheathe is attached to the center of the copper target plate and fixed by the nylon spacer. The contact area between the copper plate and the spacer is made as small as possible for suppressing heat transmission. The maximum temperature of the measurement

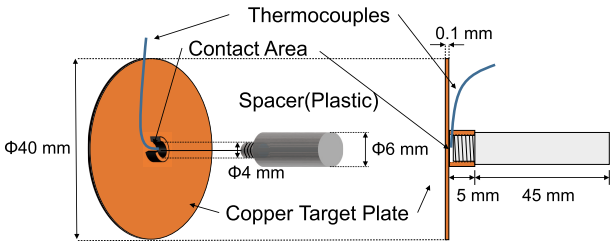

Fig. 3 Schematic image of the calorimeter.

limit is the melting point of the nylon spacer. As a result, in later experiments, the maximum incident energy is limited to 0.4 W. However, this value can be varied depending on the material of the spacer. The TC is ungrounded one, i.e. the hot junction end is electrically isolated from the SUS sheathe. Since the introduction terminal of the TC is attached on a insulation flange, the sheath is floated to the vacuum chamber. Since the sheathe is extracted to atmosphere, it is possible to measure the temperature of the target plate and the inflow current I_{in}. Figure 4 shows a constitution of measurement circuit. The ions flow into the target plate pass through from the sheathe to a ground path. They are measured as an inflow current I_{in}. When there is a temperature difference between the hot junction and the reference junction, which is inside the isolation amplifier in Fig. 4, the TC produces a temperature-dependent volt-

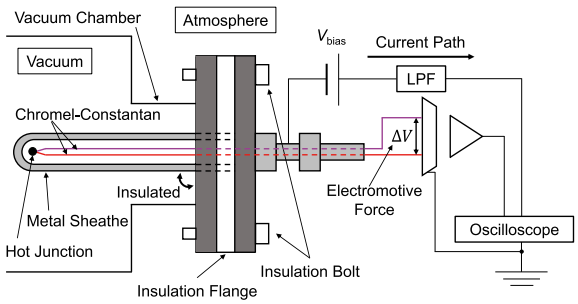

Fig. 4 Constitution of measurement circuit.

age (electromotive force). The voltage is interpreted in a different circuit from the path of the inflow current to measure temperature T.

3. Evaluation of the Heat Quantity in the PM-CuspDEC

3.1 Incident and detected rate of the heat flow

When the ions bombard the target plate, the energy of the ions is given to the target plate and the temperature of the target plate increases. In this paper, the results are evaluated by the rate of heat flow due to the variation of temperature.

Assuming total kinetic energy of the ions is converted into heat energy, the incident rate of the heat flow $\dot{Q}_{\mathrm{in}}$ from ions is evaluated simply; taking a product of the energy of ion and an inflow current as the following:

$$\dot{Q}_{\mathrm{in}} = (V_{\mathrm{ex}} - V_{\mathrm{bias}}) \cdot \frac{I_{\mathrm{in}}}{2}, \tag{1}$$

where I_{in} is divided by 2 due to the RF power source is operated by a continuous pulse with a duty ratio of 0.5. The thermal energy depending on the ion temperature can be neglected since the ion temperature is much smaller than $(V_{\mathrm{ex}} - V_{\mathrm{bias}})$.

Next, assuming the temperature distribution of the target plate can be neglected, the detected rate of heat flow $\dot{Q}_{\mathrm{det}}$ is also evaluated simply according to time variation of the temperature of the target plate as the following:

$$\dot{Q}_{\mathrm{det}} = \rho c V \frac{\mathrm{d}T}{\mathrm{d}t} \sim \rho c V \frac{\Delta T}{\Delta t}, \tag{2}$$

where ρ, c, and V are density, specific heat capacity, and volume of the copper target plate, respectively, Δt is the length of time when the CM is exposed to ions, and ΔT is the variation of temperature before and after exposure. In this experiment, Δt is equal to be 60 seconds.

3.2 Conductive and radiative losses of the rate of heat flow

Although the new CM is made to suppress the heat transmission as much as possible, the heat losses must be considered: the thermal conduction and radiation. They could be calculated according to several theorems. The

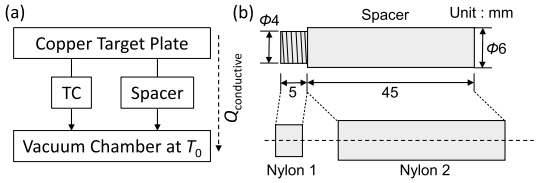

Fig. 5 (a) Considered thermal paths for calculating the conductive heat loss. (b) Simplified model of the nylon spacer in the calculation.

Table 1 Physical properties used in the calculation.

Material	k [Wm^{-1}K^{-1}]	A [mm^2]	L [mm]
TC	40	0.79	500
Nylon 1	0.22	12.56	5
Nylon 2	0.22	28.26	45

conductive heat loss $\dot{Q}_{\mathrm{conductive}}$ is evaluated by the following equation based on the law of heat conduction known as Fourier's law, so $\dot{Q}_{\mathrm{conductive}}$ can be obtained by

$$\dot{Q}_{\mathrm{conductive}} = C \cdot (T - T_0), \tag{3}$$

where C is the thermal conductance calculated by thermal conductivity k, cross sectional area A, thickness L of a thermal path, and T_0 is the temperature of the vacuum chamber. It is determined by the temperature at the start of experiment and defined as constant. Thermal paths of the conductive heat loss considered in the calculation are shown in Fig. 5 (a). The heat flux travels from the target plate to the TC and the spacer in parallel. The physical properties used for the calculation, like thermal conductivity are listed in Table 1. A part of the spacer in the thermal path is calculated as a simplified model that two nylon cylinders are connected in series as shown in Fig. 5 (b).

The radiative heat loss can be evaluated by Stefan-Boltzmann's law given as the following equation:

$$\dot{Q}_{\mathrm{radiative}} = \varepsilon S \sigma (T^4 - T_0^4), \tag{4}$$

where ε is an emissivity factor, S is the radiating surface area of the target plate, σ is the Stefan-Boltzmann constant. The total heat loss is given by the following equation: $\dot{Q}_{\mathrm{loss}} = \dot{Q}_{\mathrm{conductive}} + \dot{Q}_{\mathrm{radiative}}$.

4. Experimental Results

When the CM is exposed to helium ions, the inflow current I_{in} is measured and the temperature T of the target plate increases with the exposure time as shown in Fig. 6. In the experiment, the exposure time is set to be 600 seconds. T and I_{in} are measured in every 60 seconds. The extraction voltage V_{ex} is set to be 200 V and 100 V. The measurement with floating extraction electrode is also carried out, when the measured floating voltage is used as V_{ex}. The incident and detected rate of heat flow during 60 seconds are obtained by I_{in} and T according to equations in Sec. 3, and their averages are calculated respectively. The

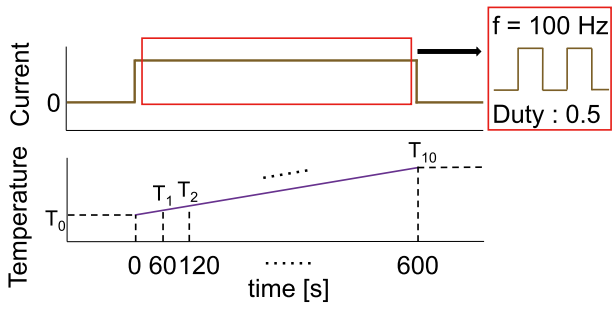

Fig. 6 The schematic image of time evolution of the inflow current and the temperature depending on the exposure time.

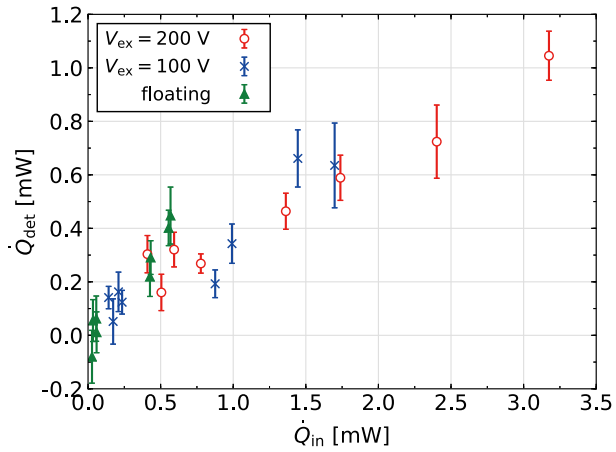

Fig. 7 The detected rate of heat flow vs. the incident rate of heat flow.

dependency on $\dot{Q}_{in}$ is measured by changing I_B since the inflow current I_{in} depends on the coil current I_B.

Figure 7 shows the detected rate of heat flow $\dot{Q}_{det}$ versus the incident rate of heat flow $\dot{Q}_{in}$. The results show that $\dot{Q}_{det}$ has a proportional relation with $\dot{Q}_{in}$. It means that the CM can detect small temperature variation due to the heat quantity on the order of mW. Figure 8 shows the dependence of the detected rate of heat flow and the evaluated rate of heat loss flow ($\dot{Q}_{det}$+$\dot{Q}_{loss}$) on the incident rate of heat flow $\dot{Q}_{in}$. The outline of the graph hardly changes, which means $\dot{Q}_{loss}$ is much smaller than $\dot{Q}_{det}$. It indicates that the new CM achieved to suppress the heat transmission.

Contrary, the slope of date points is approximately the level of 0.4, which means the CM could not detect all of the incident heat flow. Although $\dot{Q}_{in}$ is evaluated by the simple equation, it must be considered the energy reflection and the secondary electron emission on the surface of the CM since the CM composed of metal. For more accurate

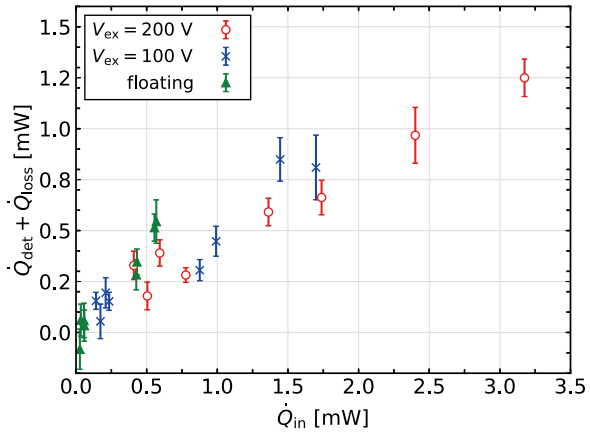

Fig. 8 The detected rate of heat flow from the experiment with the estimated heat loss vs. the incident rate of heat flow.

evaluation, they should be taken into account.

5. Conclusion

In order to measure the heat quantity in the PM-CuspDEC, a new calorimeter (CM) was manufactured and tested by helium ions. It was designed to improve sensitivity by suppressing heat transmission. Experimental results indicated that the new CM worked successfully, and detected the small variation of temperature. Taking heat losses into account, the loss of the rate of heat flow was much smaller compared with the detected rate of heat flow.

Acknowledgement

The authors acknowledge valuable discussions with Drs. J. Miyazawa and T. Goto. This work is supported by the bilateral coordinated research between Plasma Research Center, University of Tsukuba, National Institute for Fusion Science, and Kobe University (NIFS16KUGM109).

[1] H. Takeno *et al.*, Trans. Fusion Sci. Technol. **63**, No.1T, 131 (2013).
[2] H. Momota *et al.*, Proc. 14th IAEA **3**, 319 (1993).
[3] K. Nishimura *et al.*, 30th Ann. Meeting of JSPF, 04aD12P (2013) [in Japanese].
[4] Y. Nakashima *et al.*, J. Nucl. Mater. **438**, S738 (2013).
[5] Y. Nakashima *et al.*, Fusion Sci. Technol. **68**, No.1, 28 (2015).
[6] Y. Nonda *et al.*, 33rd Ann. Meeting of JSPF, 29aP85 (2016) [in Japanese].
[7] K. Ichimura *et al.*, Fusion Eng. Des. in press. DOI: 10.1016/j.fusengdes.2018.02.046.